Available online at www.sciencedirect.com

SCIENCE DIRECT®

Sedimentary Geology 185 (2006) 159–173

Sedimentary Geology

www.elsevier.com/locate/sedgeo

Lower Eocene carbonate cemented chimneys (Varna, NE Bulgaria): Formation mechanisms and the (a)biological mediation of chimney growth?

E. De Boever [a,*], R. Swennen [a], L. Dimitrov [b]

[a] *Geologie, K.U. Leuven, Celestijnenlaan 200E, 3001 Heverlee, Belgium*
[b] *Institute of Oceanology, Marine Geology and Underwater Archaeology Department, Varna, Bulgaria*

Abstract

In the area of Pobiti Kamani (Varna, northeast Bulgaria), massive carbonate cemented columns ("chimneys", up to 1.5 m diameter and 8 m high) and horizontal interbeds ($\leq$1.5 m thickness) occur in dispersed outcrops over an area of 70 km^2 within loose Lower Eocene sands. Field observations and petrographical and stable isotope geochemical characterisation of four studied locations reveal a relationship between these structures and processes of ancient hydrocarbon seepage. Column and interbed structures both consist of similar well-sorted silt- to sand-sized nummulitic host sediments, predominantly cemented by early diagenetic, low-magnesium calcite. Filamentous textures, about 10 μm in diameter and 80–650 μm long, are only locally detected within interparticle calcite cement of columns. Column samples from two sites reveal a similar, linear and inverse covariant trend of δ^{13}C–δ^{18}O values, which was interpreted as a mixing trend between two end member fluid/precipitation conditions, i.e. (1) a methane- and/or higher hydrocarbon-derived carbon member characterised by δ^{13}C values as low as −43‰ and marine controlled precipitation conditions with δ^{18}O of -1 ± 0.5‰ V-PDB and (2) a member with less contribution of methane which was mixed most likely with less depleted carbon sources explaining δ^{13}C values ranging up to −8‰ V-PDB. The corresponding, depleted δ^{18}O values, with many samples clustering around −8‰ V-PDB, are interpreted in terms of precipitation at elevated temperatures. This suggests the venting system was not a true "cold" seep, sensu stricto. Furthermore, column cross-transects often document an internal pattern consisting of (concentric) zones with distinct isotopic signatures, which vary between the two end members. The mixing and internal pattern of column isotopic data, together with petrographical observations, are qualitatively interpreted as evidence of alternating precipitation conditions, controlled by varying seepage rates of a single fluid source at depth, during build-up of individual chimney pipes near the sediment surface. Based on several field observations, migration of the hydrocarbon-charged fluids in Lower Eocene times was possibly channelled along NE oriented faults. Isotopic signatures of calcite cemented horizontal interbeds, with depleted δ^{18}O ratios as low as −8.88‰ V-PDB and variable δ^{13}C (−1‰ to −16‰, mainly around −5‰ to −7‰) suggest that ascending fluids contributed to their cementation or resetted the calcite cement isotopic signature, predominantly during periods of active seepage of warmer fluids. Only few petrographical (and preliminary lipid-biomarker) evidence has been found, pointing to the presence or possibly former activity of microbiota, involved in carbon cycling and calcite precipitation, typical of cold seep settings. This may result from diagenetic alteration of organic components. However, considering

* Corresponding author. Katholieke Universiteit Leuven, Afd. Geologie, Celestijnenlaan 200E, B-3001 Heverlee, Belgium. Tel.: +32 16 327798; fax: +32 16 327983.

E-mail address: eva_deboever@yahoo.com (E. De Boever).

doi:10.1016/j.sedgeo.2005.12.010

the processes of chimney formation, a cementation process, governed by the inorganic oxidation of hydrocarbons in which interstitial oxygen is rapidly consumed without bacterial mediation, is considered.

Keywords: Authigenic carbonates; Cold seep; Methane oxidation; Eocene; Varna; Bulgaria

1. Introduction

Within the past decade, an increasing number of submarine locations of hydrocarbon seepage, often associated with characteristic chemosymbiotic invertebrates and carbonate deposits has been identified. Many of them have been intensively studied in order to understand the mechanisms of fluid venting and carbonate cementation. Furthermore, based on typical features defined in modern settings, fossil seep carbonates have been discovered in the geological record (Peckmann et al., 1999, 2002; Clari and Martire, 2000; Campbell et al., 2002; Clari et al., 2004). Studying these fossil records of hydrocarbon seepage can further contribute to our knowledge and understanding of venting processes and carbonate diagenesis at modern and fossil equivalents.

Seep carbonates are a well-known product of cold seeps. It is assumed that upward migrating methane and other gases, often channelled along permeable horizons such as fault planes, are oxidized near the sea floor yielding patchily distributed outcrops of carbonate cemented structures, ranging from small slabs, concretions, doughnut-like structures to large chimneys (Hovland et al., 1987; Ritger et al., 1987; Jensen et al., 1992; Jorgensen, 1992; Sakai et al., 1992; Peckmann et al., 2001; Díaz-del-Río et al., 2003). They form a fossil record of hydrocarbon-rich fluid expulsion and especially the stable isotopic composition of early diagenetic carbonate cements has been intensively studied as a window to the identification of the hydrocarbon source and precipitation conditions (Greinert et al., 2001; Peckmann et al., 2001; Campbell et al., 2002).

The typical low δ^{13}C signature (down to -80‰ V-PDB) of these deposits is due to the incorporation of methane- and/or higher hydrocarbon-derived carbon. When seepage rates are high enough, fluids can reach the sea floor where they are oxidized in aerobic conditions and may be actively expelled into the water column (Hovland et al., 1987; Aloisi et al., 2000; Peckmann et al., 2001). In the presence of free oxygen, aerobic methanotrophs can thrive on methane and produce CO_2 (Cavagna et al., 1999). When fluid seepage is slower, hydrocarbons are assumed to be effectively oxidized anaerobically within the sediment column by a coupled process of bacterial mediated sulphate reduction and methane oxidation (Hoehler et al., 1994; Aloisi et al., 2000). This coupled process increases levels of alkalinity and dissolved inorganic carbon (DIC) in the pore fluids, in this way favouring carbonate precipitation (Ritger et al., 1987; Aharon, 2000).

Some peculiar petrographic fabrics, such as filamentous textures and micritic cloths, enveloped within the carbonate cements have been interpreted as evidence of such fossil microbial activity in possible relation to seepage of hydrocarbons and/or other gases (Cavagna et al., 1999; Peckmann et al., 2001, 2002). In addition to petrography, molecular and stable isotope analyses have been able to identify the chemolithotrophic bacteria mediating the process of carbonate precipitation at cold seep settings, although the exact biogeochemical pathways are still not fully understood (Hoehler et al., 1994; Thiel et al., 1999; Boetius et al., 2000; Peckmann and Thiel, 2004).

We report here on the carbonate cemented structures of the Pobiti Kamani area, located near Varna (northeast Bulgaria). The area envelops several dispersed outcrops of massive, carbonate cemented vertical columns and horizontal interbeds contrasting with the loose surrounding sandy sediments. Morphological similarities with present-day forming seep-deposits in the northwestern Black Sea (Thiel et al., 2001; Michaelis et al., 2002; Peckmann et al., 2002) and abundant hydrocarbon seepage along the nearby Bulgarian coast (Dimitrov and Dontcheva, 1994; Dimitrov, 2002) have led to the hypothesis of a cold seep-related origin. Only a single preceding study has prudently addressed this hypothesis, based on a limited set of stable isotope data (Botz et al., 1993). However, the structures of the Pobiti Kamani are unique both regarding their good preservation, abundance (locally over 100 columns in a single outcrop) and immense dimensions. We present here newly gathered petrographical and a large set of stable isotope data of column and horizontal interbed structures from four locations which were studied during a first reconnaissance field trip. This study focuses on the processes controlling the formation of these structures and the question on the (micro)biological mediation of carbonate precipitation.

2. Geological setting

The Pobiti Kamani area is situated 18 km west of Varna, on the eastern end of the Moesian Platform near the Black Sea coast (Fig. 1A). The tectonic evolution of Bulgaria and the western Black Sea has been discussed by Foose and Manheim (1975); Hsü et al. (1977); Doglioni et al. (1996) and Bergerat et al. (1998). The Moesian Platform comprises the northern half of Bulgaria, extending towards Romania, and generally consists of gently south-east dipping Paleozoic to Cenozoic sedimentary sequences. Since Hercynian tectonic activity the platform has been relatively stable, except for repeated fault reactivations in the east, due to both compressional and extensional Alpine tectonogenesis, which affected the Black Sea area from the Late Triassic onwards. The resulting block-faulted pattern of the eastern Moesian Platform, characterizes also the present-day deeper structure of the Pobiti Kamani area. In general, two main fault systems are distinguished

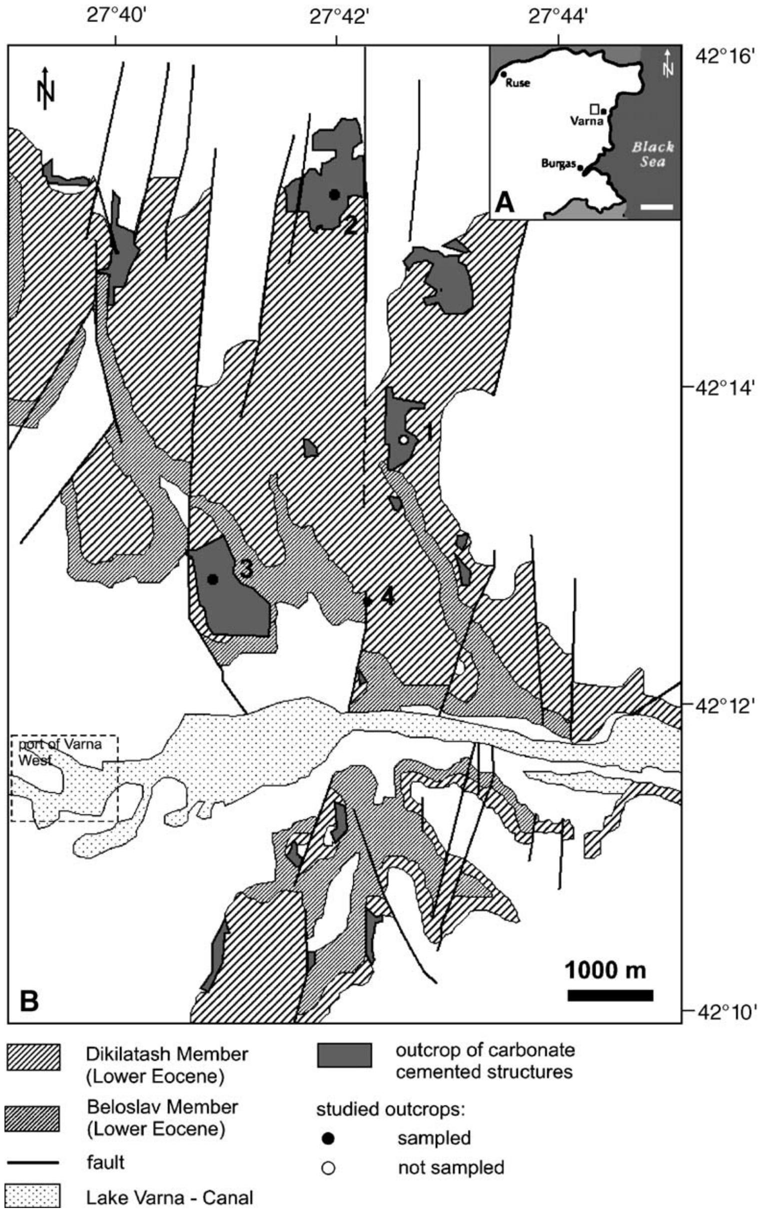

Fig. 1. Study area. (A) Location of the area of study, 18 km west of Varna (square not to scale). Scale bar = 50 km. (B) Area of Pobiti Kamani with indication of the dispersed outcrops of carbonate cemented structures and the four studied locations. 1 = Main Group, 2 = Slunchevo north, 3 = Beloslav Quarry, and 4 = Beloslav north. Unpatterned areas are Lower-Cretaceous to Quaternary sediments.

(Georgiev, personal communication), i.e. (1) an east–west trending system characterized by normal and reverse faulting and (2) a north–south oriented system of normal and strike-slip movement. During Paleogene times NNW–SSE and NNE–SSW oriented extensional tectonics predominated, which resulted in a set of step faults (east side down) towards the western Black Sea, with most rapid subsidence during Oligocene–Miocene times.

The Lower Eocene sedimentary sequence in the area of Pobiti Kamani consists of limestone and quartz sands to sandstone of the Dikilatash Member (~50 MA), overlying marly deposits of the Beloslav Member (Fig. 1B). The sedimentary conditions during deposition of the Dikilatash sands consisted of a shallow, about 70 m deep, epicontinental sea, characterized by littoral to neritic depositional conditions. This is reflected in sandy deposits in the north, which grade into more silt-sized sediments, interlain by nummulite-rich horizons to the south. The nearshore current activity resulted in the well-sorted nature of the sands. The Dikilatash Member reaches a thickness of about 40 m and hosts the carbonate cemented structures (Fig. 1B). At least 18 isolated outcrops of less than 0.2 up to 1.5 km in length, are presently exposed, scattered over a 70 km^2 large area. Four locations are addressed here, i.e. the Main Group, the Beloslav Quarry, Slunchevo north and the Beloslav north site.

3. Field observations

The most impressive carbonate cemented structures observed in the studied outcrops (Fig. 1B) are vertical, cylindrical columns and subhorizontal cemented interbeds, which both appear to consist of carbonate cemented portions of the sand–silt-sized, nummulite-rich host sediment.

The cylindrical columns normally reach heights from 1 to about 4 m, but sometimes they are up to 8 m high and have diameters up to 1.5 m (Fig. 2A). Other shapes such as cones and cylinders with a mushroom-like top also exist. Most of them are still in vertical position however fragments of eroded, fallen structures also occur (Fig. 2A, B). They possess a subcircular cross-section often with a decreasing degree of carbonate cementation towards the centre which is regularly marked by a single or double, irregular hollow tube (Fig. 2B), sometimes with evidence of bioturbation, or filled with loosely cemented sand which is identical to that of the host sediment. The column surface is either rather smooth or is often found to be more irregular with evidence of bioturbation (Fig. 2C). The contact with surrounding loose sands is dominantly sharp, but may locally be more gradual. At the Main Group, columns occur in two clusters each comprising up to hundred individual columns (Figs. 1B and 2A). In vertical section, the columns are organized in five main "levels", which is exposed at the Beloslav Quarry (Figs. 1B and 2D) where a 40 m thick section is visible and columns are NS aligned along the vertical wall. These levels of columns are separated by horizons of horizontal carbonate cemented interbeds (Fig. 2C, D), each up to 1.5 m thick. The distribution of horizontal interbeds seems to be restricted to areas near locations of vertical column development. Local modifications of the columns, such as bifurcations and lateral offset of columns in successive levels, occur in correspondence with these horizontal interbeds. However, single columns can also often be followed, crosscutting one or more horizontal interbeds. At the base of the Beloslav Quarry the lowermost level (level 1) is distinct from the higher level interbeds due to its large areal extent. This ± 0.5 m thick, nummulite-rich horizon has been interpreted as a marine hardground horizon and defines the base of the Dikilatash Member (Nacev et al., 1986).

A major normal fault contact between Upper Cretaceous marl and the Dikilatash sands at the Beloslav north outcrop (Figs. 1B and 3), trends along a N6E56E direction. The cemented Dikilatash sands of the hanging wall form a well marked topographic elevation. Only one smaller column is presently located close to the fault. Away from the position of the fault, the degree of cementation of the sands rapidly decreases over a distance of about 50 m. The orientation of the Beloslav north fault, as well as the NS alignment of columns at the Beloslav Quarry, both coincide with the $\pm$NS direction of extensional faulting during Paleogene times in the eastern Moesian Platform and in this respect support a structural control of active regional faulting on the distribution of carbonate cemented structures.

4. Methods

Samples of columns and cemented interbeds were collected from three locations (the Beloslav Quarry, Slunchevo north, Beloslav north). The Main Group is situated in a touristic park. Hence structures could not be sampled at this location. Special attention was paid to the sampling of columns of which one or two cross-transect(s) were hand-drilled. This allowed to evaluate petrographical and geochemical changes during column growth. Standard thin sections were examined by conventional transmitted, reflected and UV light microsco-

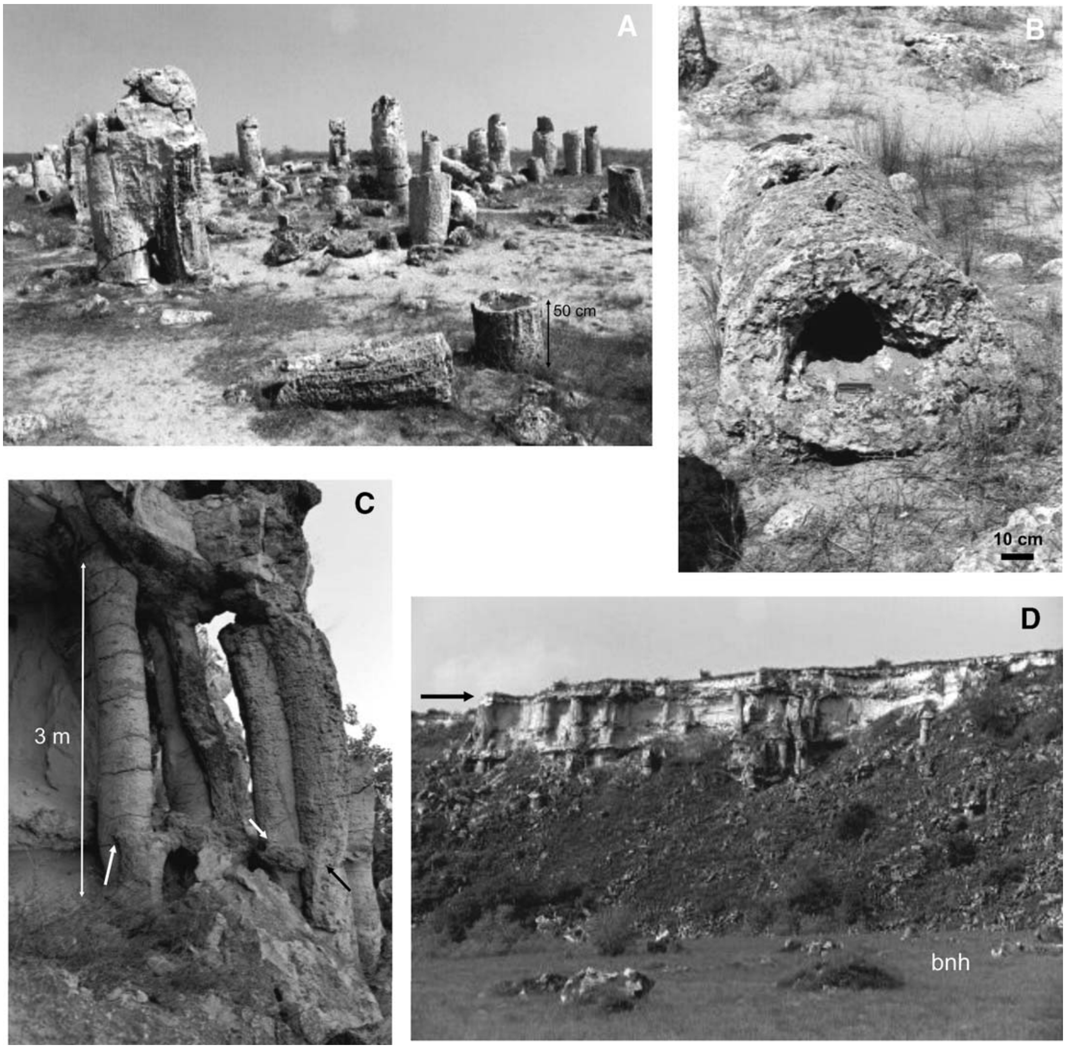

Fig. 2. Carbonate cemented columns and horizontal interbeds. (A) Cluster of vertical columns at the Main Group outcrop with cemented horizontal interbed at their base. Notice also the presence of scattered fragments of broken columns. (B) Cross-section of column with central open conduit. Scale bar = 10 cm (Main Group). (C) At the point of contact, columns either cross the horizontal interbed (white arrows) while the others seem to intergrow with the interbed (black arrow) (Beloslav Quarry). (D) Overview of part of the Beloslav Quarry with two levels of carbonate cemented columns, separated by horizontal interbeds (arrow points to level 5). Bnh = Basal nummulite-rich hardground (level 1). The wall is about 40 m high.

py. Samples were impregnated with blue epoxy in order to visualize the porosity distribution. Eight samples were stained with a mixture of Alizarin red and Potassium-ferricyanide to deduce carbonate mineralogy and presence or absence of ferroan phases. As all carbonate phases turned out to be non-ferroan, low-magnesium calcite, no additional samples were stained. Three, 100 μm thick thin sections were prepared to evaluate the existence of larger bacterial filamentous textures. Point counting (Galehouse, 1971) was carried out, following the Glagolev–Chayes method, in order to quantify the amount of cement versus detrital/biogenic fragments and porosity. Cathodoluminesence studies were carried out using an in-house built cold cathode luminescence instrument to further refine cement characteristics. A Jeol JSM 6400 scanning electron microscope was used for detailed studies with high magnification (×100.000) of slightly etched (0.1 M HCl, 1 min) gold coated broken rock chips. In this study SEM was particularly applied to search for microbial textures. Sampling for stable C and O isotopes was carried out with a hand-held microdrill. Samples preferentially were taken far from loose, weathered parts and few centimetres below the top of the drilled plugs. Because of the abundance of foraminifera in the cemented sandstones, the incorporation of shell material in

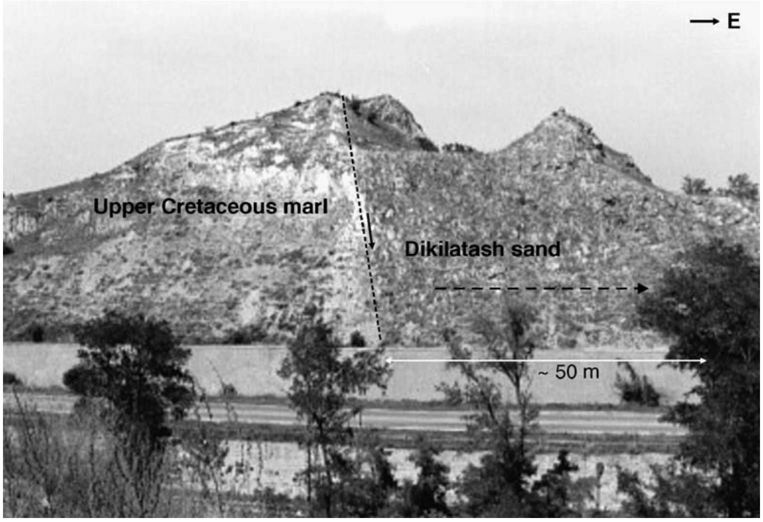

Fig. 3. Beloslav north outcrop with major normal fault contact between sands of the Dikilatash Member and Upper Cretaceous marly sediments. Dashed arrow indicates direction of decreasing degree of carbonate cementation of the Dikilatash sands, away from the fault.

some of the samples could not be completely avoided; however care was taken to reduce this interference to a minimum. δ^{13}C and δ^{18}O results are reported relative to the V-PDB standard. Isotope measurements were carried out at the Laboratory of the University of Erlangen (Dr. Joachimsky) where carbonate powders were reacted with 100% phosphoric acid (density <1.9 g/cm^3, Wachter and Hayes, 1985) at 75 °C using a Kiel III online carbonate preparation line connected to a ThermoFinningan 252 massaspectrometer. Sol II and NBS 19 isotope standards were used. The standard deviation for δ^{13}C was 0.02‰ V-PDB and 0.06‰ V-PDB for δ^{18}O.

5. Results

5.1. Petrographical description of columns and horizontal interbeds

Both columns and horizontal interbeds consist of, at present, (low-magnesium) calcite cemented, sub-arkosic sandstone which is grain-supported with a calcite content varying between 29 and 39 vol.%, thus pointing to early diagenetic cementation prior to significant burial and compaction (Fig. 4A–C). In interbeds, interparticle micrite may reach up to 5 vol.%, even up to about 10 vol.% in the basal nummulite-rich hardground. Sand- to silt-sized, well-sorted quartz and feldspar grains reach up to 48 and 9 vol.%, respectively. Glauconite, muscovite flakes, zircon, tourmaline, sphene and rutile grains, detrital clays and minor detrital carbonate particles are present with a total content always below 5 vol.%. Feldspar grains are often altered, showing a light brown colour, or they are partly transformed to dark coloured clays (most likely illite). Corrosion of feldspar locally also gave origin to minor secondary porosity. The typical straight outline of muscovite flakes indicates that the sandstones did not undergo strong compaction before cementation. Opaque ellipsoidal to irregularly shaped minerals consist of detrital ilmenite. Despite a thorough search for authigenic pyrite phases, no sulphides were found within the studied samples. Also their possible weathering products, i.e. Fe-oxy/hydroxides were few.

The most important biogenic components are tests of small and large foraminifera (about 20 vol.%, Fig. 4A–C), dominantly Alveolina and Nummulitidae. They sometimes have been broken during transport, prior to the infill with micrite and detrital particles (Fig. 4C). *N. striatus*, *N. behumoni* and minor *N. bombitus* have been determined (Baccaert, personal communication). Most bioclasts possess a bright (spotted) luminescence (Fig. 4B, D), which is indicative of (partial) recrystallization. Besides foraminifera, minor single corals were found.

In total, 4 cement phases were identified of which the second mentioned is the most abundant (Figs. 4 and 5), i.e. (i) non-luminescent–bright luminescent, zoned dogtooth cement (DC), (ii) interparticle dull luminescent equant calcite (EC1), (iii) dull luminescent, transparent equant cement in small keystone-type of vugs (ECk) and (iv) equant calcite cement with a characteristic non-luminescent–bright luminescent zoned pattern (EC2). Dogtooth cements (DC,<1.5 vol.%) were found within column samples, but this cement type most

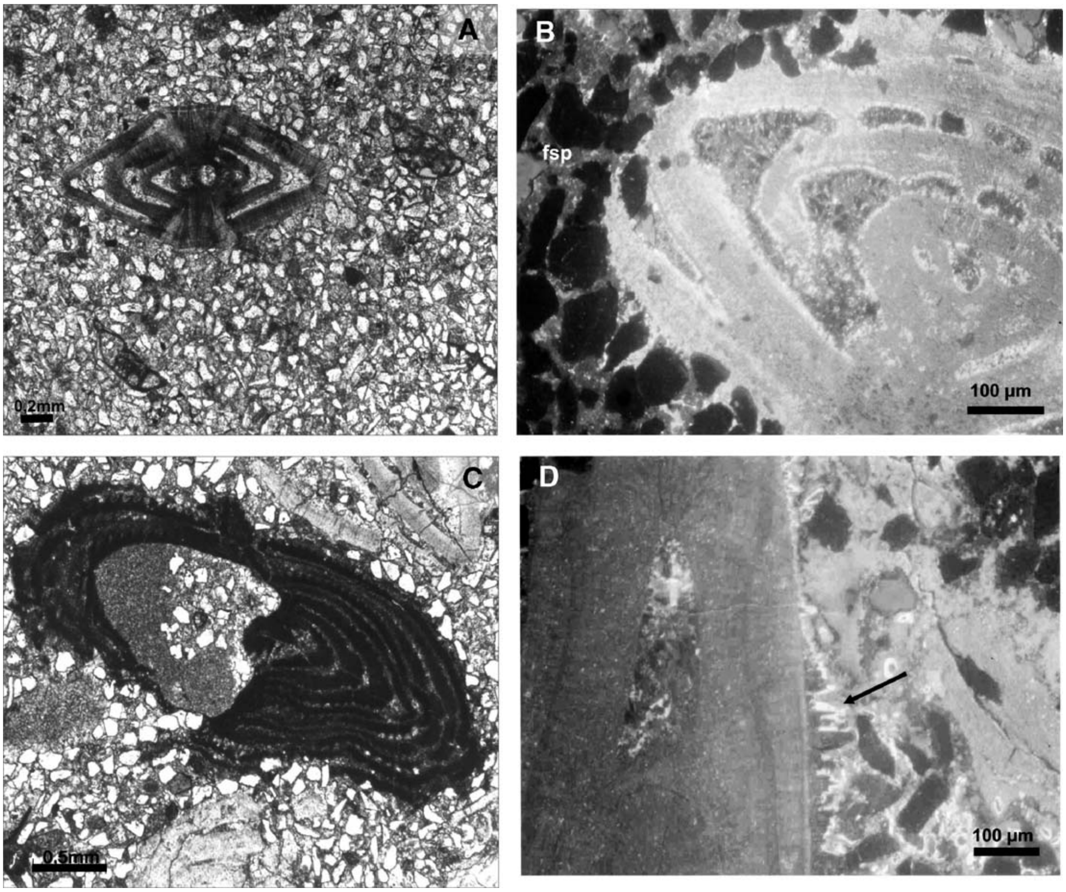

Fig. 4. Petrography of the sandstone structures. (A) Microscopic texture of column sample: calcite cemented (EC1) sandstone, enveloping small and large foraminifera and dominance of quartz grains. Opaque grain corresponds to detrital ilmenite. (B) Dull luminescent, interparticle EC1 cement with scattered fine bright luminescent spots (recrystallization?) and bright luminescent, likely recrystallized large foraminifer. Quartz grains are non-luminescent. fsp = Feldspar grain. (C) Test of Alveolina, partly eroded prior to sedimentary infill with detrital grains and micrite (horizontal interbed sample). (D) Non-luminescent–bright luminescent zoned dogtooth cement (arrow), surrounding a nummulite test (horizontal interbed sample).

clearly developed in horizontal interbeds. The dogtooth-shaped crystals are substrate selective, discontinuously surrounding foraminifera. They exhibit a non- to orange-yellow bright cathodeluminescence zonation pattern (Fig. 4D). Interparticle as well as intraforaminifer porosity, and porosity along fine, irregular fractures subsequently became cemented by subhedral, equant low-magnesium calcite crystals, generally 20 to 120 μm in diameter (EC1) (Figs. 4A–C and 5A). Luminescence characteristics of this cement phase can vary, but crystals are dominantly dark brownish, dull luminescent within column samples (Fig. 4B). Locally, dull luminescent cements with bright spots may be suggestive of some limited degree of recrystallization. Interparticle cementation of horizontal interbeds generally exhibits luminescence characteristics similar to the ones of EC1 column cements; however, here also dull to non-luminescent equant calcites as well as “poikilotopic” phases occur. In some horizontal interbeds, micrite occurs in primary porosity and exhibits similar cathodeluminescence characteristics as EC1.

Several millimetre-large cavities, cemented by transparent, equant calcite crystals, 0.2 to 1 mm in diameter (ECk, about 1.5 vol.%) occur in the fifth horizontal interbed level (Figs. 2D and 5A). Noteworthy is that the cemented cavities are larger than the mean interparticle porosity size and thus can best be described as oversized pores. Their systematic occurrence in what seem to be sheltered positions below foraminifera (Fig. 5A), which can be inferred from the geopetal sediment infill within the foraminifera chambers, suggest a kind of “keystone”-type origin of these vugs, where cavities relate to entrapped gas phases which subsequently have been cemented. An alternative explanation is that the cavities correspond to secondary pores, created by alteration of aragonite bioclasts, but this would not

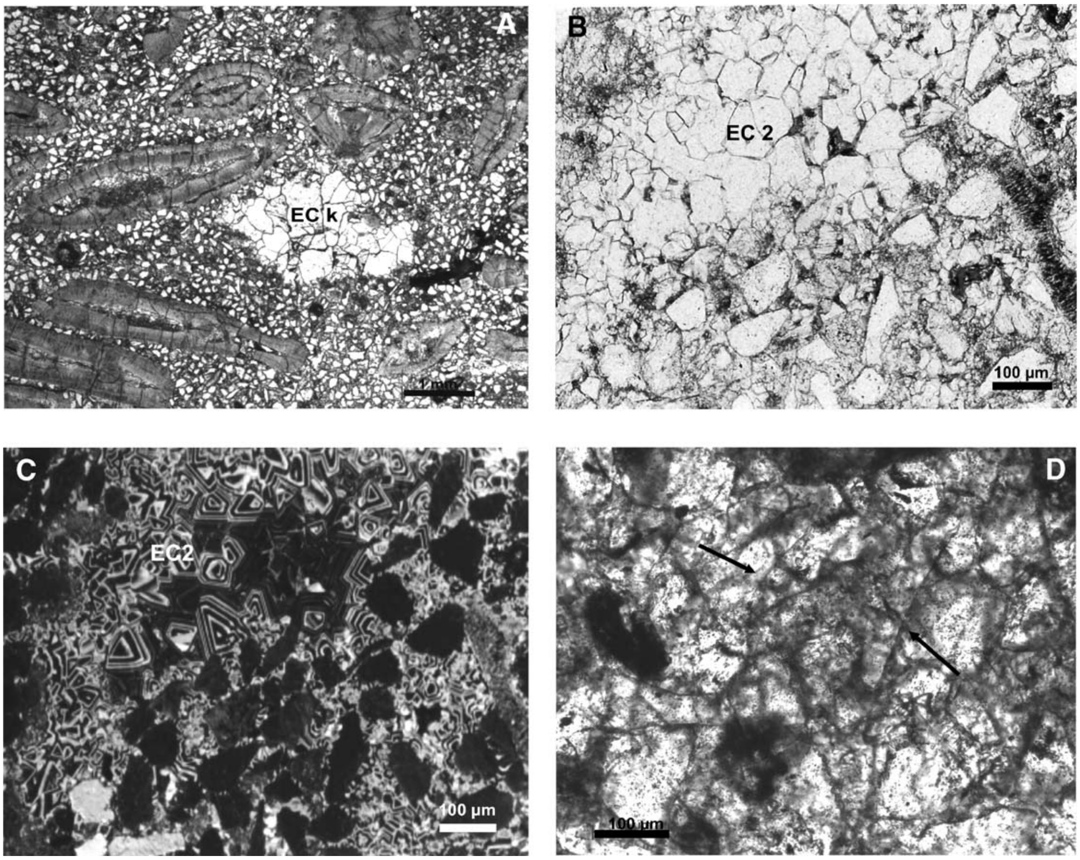

Fig. 5. Petrography of the sandstone structures–calcite cements. (A) Large vug between foraminifera tests, cemented by 0.2–1 mm diameter, equant calcite crystals (ECk) in horizontal interbed sample. Note the geopetal infill of micrite in several foraminifera chambers. (B) Biomold cemented by equant calcite cement (EC2) in horizontal interbed sample. (C) Same view as (B) with cathodeluminescence light, revealing the non-luminescent–bright luminescent zonations of EC2 calcite crystals. (D) Rare example of fine, dark filaments (arrows), overlying several quartz grains and enveloped within interparticle column calcite cement (EC1).

explain their sheltered position. At last, transparent sub- to euhedral, equant shaped calcite crystals constitute the fourth cement type (EC2,<1 vol.%) and incompletely fill secondary biomoldic porosity (Fig. 5B) and enlarged fractures crosscutting cemented host rock. Clearly distinguishable and repeated non-luminescent–bright luminescent zonations (Fig. 5C) support variable redox conditions during crystal growth, at least if these zonations correspond to variations in Fe and Mn content (Barneby and Rimstidt, 1989). This is characteristic of precipitation in the meteoric realm. Present-day porosity is small and in the order of 3% bulk volume, is predominantly of secondary origin and mainly relates to biomolds and the dissolution of detrital feldspar grains.

Accumulations of fine, dark brown filaments, 80 to 650 μm long and about 10 μm diameter, were very locally found within column-derived thin sections, but not by SEM. Filaments are overlying detrital grains and enveloped within EC1 (Fig. 5D). These filaments reveal a strong yellow-green fluorescence. They occur either as distinct individual filaments overlapping each other randomly or they are arranged in dense clusters of parallel lying strings. Despite SEM study of several HCl (0.1 M) etched column-derived samples, these filaments could not be traced. Similar textures have not been recognized in the basal nummulite-rich hardground. Their absence or presence within the other levels of cemented horizontal interbeds compared to columns, should be further investigated.

5.2. Carbon and oxygen stable isotope analyses of columns and horizontal interbeds

Based on negative δ^{13}C values as low as −29‰ V-PDB for a column-derived sample Botz et al. (1993) suggested that a carbon source, linked to the degradation of organic matter was likely and possibly also a contribution of oxidized methane could be taken into account. Recorded isotopic values within the more than 150 samples analysed in this study, were as low as – 43‰ V-PDB for the column calcite cement (EC1). The latter values fall within the range of values reported from modern and ancient cold seep carbonates (Clari and Martire, 2000; Peckmann et al., 2001, 2002; Campbell et al., 2002; Díaz-del-Río et al., 2003), thus confirming the incorporation of methane and/or higher hydrocarbon-derived carbon.

The carbon–oxygen isotopic cross-plot of all column-derived samples is presented in Fig. 6. They were collected from three different areas, i.e. a single sample for the column along the Beloslav north fault and in total seven columns at Slunchevo north and the Beloslav Quarry. The dataset reveals two similar, negative covariant, linear trends for the samples from Slunchevo north and the Beloslav Quarry. $\delta^{18}O$ ratios range from around $-1 \pm 0.5‰$ V-PDB down to $-9‰$ V-PDB, linked to increasing $\delta^{13}C$, shifting from $-25‰$ till $-8‰$ V-PDB. At the end of the linear trend, characterized by least depleted oxygen isotopic ratios, excursions in $\delta^{13}C$, down to $-43‰$ occur. Isotopic ratios thus indicate a mixing system of two end member compositions, namely strongly depleted $\delta^{13}C$ associated with least depleted $\delta^{18}O$ on the one hand and least depleted $\delta^{13}C$ ratios together with most depleted $\delta^{18}O$ ratios on the other hand.

When looking into more detail along individual column transects, the covariant carbon–oxygen isotopic trend recorded in a single column, often also exhibits an internal pattern in which data-clusters of the two end member compositions alternate. In Fig. 7, data of a column from Slunchevo north are presented, which was sampled along two mutually perpendicular transects. A concentric nature of the internal pattern is apparent (Fig. 7A, B). In total, four zones of distinct isotopic signature can be differentiated. Transitions between the extrema along the transect are in general sharp (Fig. 7C, D). The most depleted $\delta^{13}C$ ratios occur in the centre of the column (zone I), which is not of equal diameter along both transects, resulting in the asymmetric shape of the zones. Zones II and IV possess less depleted $\delta^{13}C$ and more depleted $\delta^{18}O$ values. Zone III consists again of relatively less depleted $\delta^{18}O$ and more depleted $\delta^{13}C$ ratios, but here the negative carbon isotopic excursion is less expressed as in zone I. Isotopic ratios, especially for carbon, within a single zone may differ by about 5‰ along the different transects (see zone III Fig. 7C, D), indicating some variability in fluid characteristics and/or precipitation conditions during the cementation of a single concentric zone. In general, the presence of such a concentric pattern is indicative of strongly varying fluid characteristics/precipitation conditions during the (concentric)

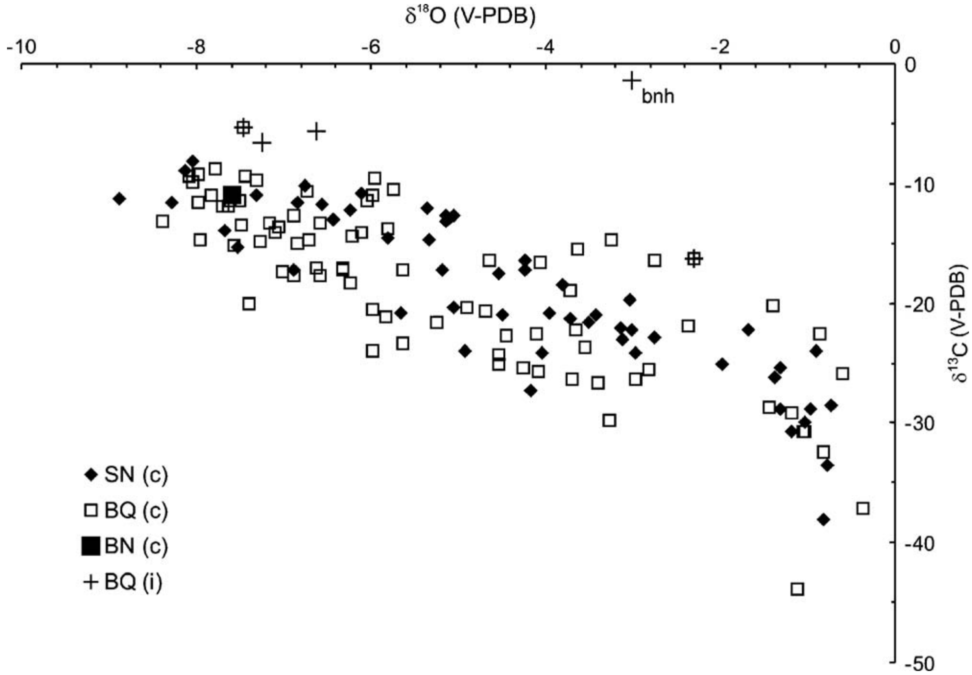

Fig. 6. Carbon–oxygen isotope plot of columns and interbed samples from three sampling locations. SN = Slunchevo north, BQ = Beloslav Quarry, BN = Beloslav north. (c) = Column sample, (i) = Interbed sample. bnh = Basal nummulite-rich hardground.

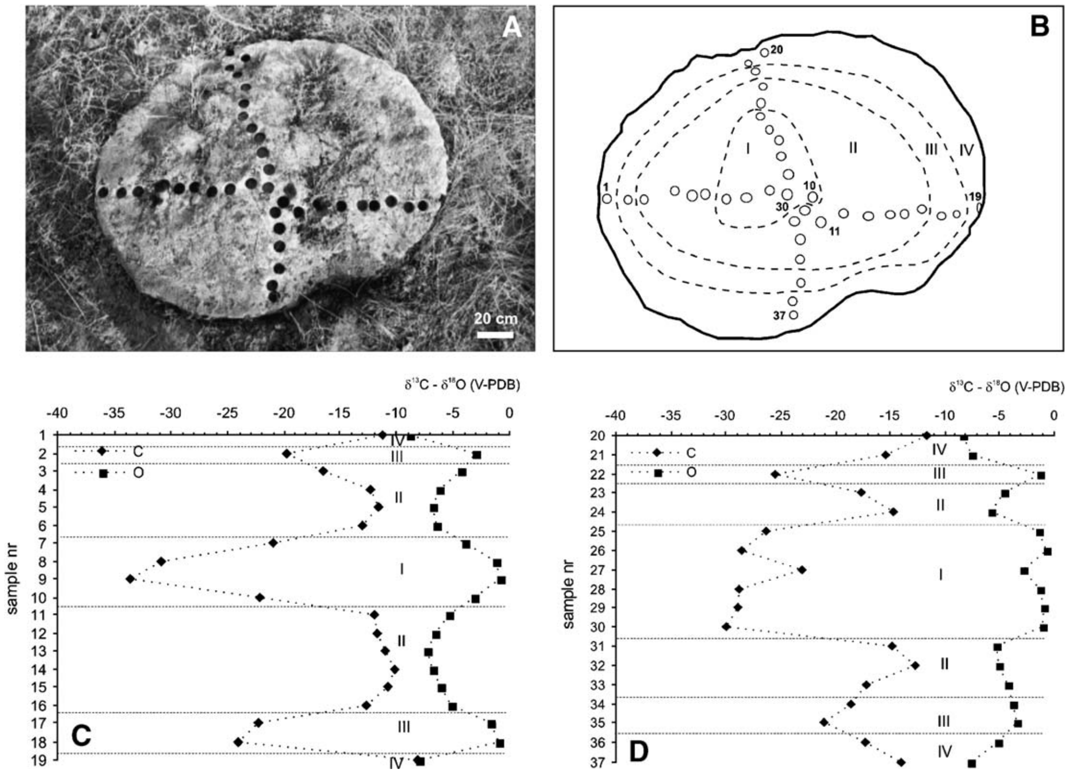

Fig. 7. Carbon–oxygen stable isotope data of a single column, subsampled along two mutually perpendicular transects (Slunchevo north). (A) Picture of the column. Circular drill holes show the position of the subsamples. (B) Drawing of column with indication of subsamples and concentric zones of distinct isotopic signatures from centre (zone I) to rim (zone IV). (C) Plot of $\delta^{13}C-\delta^{18}O$ data of subsamples 1 to 19. (D) Plot of $\delta^{13}C-\delta^{18}O$ data of subsamples 20 to 37. Delineation of the four zones of distinct isotopic signature (I to IV) is indicated in (C) and (D).

build-up of columns. In contrast to the trend in stable isotope signatures, no such pattern was obvious from (cathodeluminescence) petrography.

The internal, zoned pattern is not as well pronounced for all sampled columns. Sometimes, internal isotopic variations are smaller, whereby the $\delta^{13}C$–$\delta^{18}O$ ratios cluster of subsamples in the middle of the linear mixing trend (Fig. 6), the concentricity can be less clear or highly asymmetric. For other columns, the position of the distinct internal isotopic zones may differ along the column transect.

The majority of four studied horizontal interbed samples from the Beloslav Quarry, plot in a relatively small cluster with $\delta^{13}C$ values from −3.75‰ to −7.04‰ and $\delta^{18}O$ values ranging from −6.63‰ to −11.6‰ V-PDB (Fig. 6). However, also $\delta^{13}C$ values as low as −16.23‰ and $\delta^{18}O$ of −2.30‰ V-PDB were recorded. The recorded carbon and oxygen isotopic ratios do not represent marine precipitation conditions at ambient sea floor temperatures, as would be expected for classical marine hardgrounds (Bathurst, 1975), but indicate that cementation/recrystallization processes of the horizontal interbeds in the Pobiti Kamani area is more complex. Finally, the isotopic ratios measured for the basal nummulite-rich hardground (bnh) slightly differ from the cluster with −1.36‰ for $\delta^{13}C$ and −3.02‰ V-PDB for $\delta^{18}O$, and plot close to the Lower Eocene (~50 MA) marine carbon–oxygen isotopic signature (Fig. 6, Zachos et al., 1993).

6. Discussion

6.1. Formation of the carbonate cemented sandstone structures

The focus in this discussion will be on the EC1 cement, which is preceded by minor amounts of non-luminescent–bright luminescent zoned dogtooth cement. The latter possibly is marine in origin (Flügel, 2004). Several observations suggest EC1 calcite cementation of the structures took place at shallow depth within the sediment pile. Firstly, the high original porosity up to 39 vol.% of cemented columns and of similar magnitude in interbeds, indicates cementation occurred prior to significant burial. Secondly, the calcite mineralogy of all authigenic, early diagenetic cements is generally interpreted as an indication for carbonate precipitation near the seafloor, in aerobic conditions, where sulphate concentrations are too high for dolomite to form (Burton, 1993; Cavagna et al., 1999; Stakes et al., 1999). The absence of a petrographical indication, within the studied samples, for authigenic pyrite or other reduced sulphide phases is put forward as an additional argument for the more oxic precipitation conditions. Pyrite is frequently reported as a typical by-product of carbonate precipitation at cold seeps, resulting from the coupled process of methane oxidation and sulphate reduction in anaerobic conditions (Aharon, 2000; Peckmann and Thiel, 2004). Its absence can however also be explained by the lack of reactive iron in the system. Petrography of the Pobiti Kamani structures revealed the non-mature nature of the Dikilatash host sands with abundant corroded feldspar grains and the presence of interstitial clays which should have acted as a source of Fe, Mn, and other ions. Consequently, the lack of Fe availability is excluded as an alternative explanation for the absence of pyrite.

The range of δ^{13}C compositions of column calcite cement, with values varying approximately between –8‰ down to –43‰ V-PDB confirm that these cements partly derived from the oxidation of methane and/or higher hydrocarbons. The most negative carbon isotopic ratios mainly cluster around −25‰ to −30‰ V-PDB, plotting within the range of a thermogenic hydrocarbon-derived carbon source. However values as low as −43‰ suggest also the contribution of methane of biogenic origin. Corresponding δ^{18}O values of ±−1‰ V-PDB, testify of calcite precipitation in equilibrium with Lower Eocene seawater (Zachos et al., 1993). Furthermore, the linear, inverse covariant carbon–oxygen isotopic trend of chimney samples and the internal (concentric) pattern of the isotopic dataset along chimney-transects, point to a more complex mixing system between two end member fluids/precipitation conditions, which are of varying importance during the build-up of individual chimney pipes.

The second end member system yielded less depleted δ^{13}C values, as low as −8‰, showing that methane is not the only carbon source. Possible less depleted carbon sources are marine dissolved inorganic carbon (DIC, δ^{13}C around 0‰ V-PDB) and CO_2 generated in equilibrium with methane, possessing δ^{13}C ratios of +10‰ to +15‰ (Hudson, 1977). At the same time, the more depleted δ^{18}O ratios of −7‰ to −8‰ V-PDB have to be explained. At first, recrystallizaion or precipitation of the calcite cements, either from meteoric fluids or under elevated temperature conditions during deep burial (Botz et al., 1993), can be considered. However, no petrographic evidence of recrystallization was observed and it is highly unlikely that such a process would only partly reset local isotopic ratios, not homogenizing the observed concentric patterns. Furthermore, deep burial calcite precipitation is contradictory with the indications of cementation in near sediment surface conditions, as outlined above. Alternatively, oxygen isotopic depletions can result from the in situ, near seafloor, precipitation out of a warm, ascending fluid. The real isotopic signature of this (deep-sourced?) warm fluid is unknown, but, using the oxygen signature of Lower Eocene seawater, i.e. −1‰ V-PDB (Zachos et al., 1993) as an approximation and assuming no later resetting, temperature shifts of almost 50 °C are required to explain the δ^{18}O range, down to about −9‰ V-PDB. A similar reasoning of precipitation from deep-sourced, rising hydrothermal fluids was applied by Kulm and Suess (1990) to explain the depleted oxygen isotopic ratios of cold seep carbonates at the Oregon Accretionary Prism.

It is unlikely that these two end members resulted from the mixing of two separate fluid sources, migrating along the same fluid conduit system or a system in which a colder, upward migrating methane bearing fluid mixed with surrounding (warm) pore water as was proposed by Sakai et al. (1992) for cross column isotopic gradients. A qualitative model is proposed here, in which fluid geochemistry giving rise to calcite cementation, is controlled by the seepage rate of a single hydrocarbon-charged fluid source at depth, which varied during the build-up of individual chimneys, and in this way determined calcite precipitation temperatures and the possibility to oxidize the ascending hydrocarbons. Under conditions of, in relative terms, slow ascend of hydrocarbon-charged fluids, temperature equilibration and mixing with surrounding, cooler marine pore waters yielded δ^{18}O values close to the Lower Eocene (~50 MA) marine signature (Zachos et al., 1993). Upon passage through the sediment column, methane and/or higher hydrocarbons had enough time to become efficiently oxidized, thus yielding cements characterized by strongly depleted carbon ratios. In contrast, during stages of high rate fluid expulsion, no complete temperature equilibration was reached between seepage fluids and surrounding pore waters. As a consequence, expulsed fluids remained warm. The higher the seepage rates, the higher the near seafloor temperatures were raised and, accordingly, the lower the oxygen isotopic signature of early diagenetic calcite cements. A factor which could have enhanced relative rapid carbonate precipitation under these conditions, is the heating of interstitial colder marine waters due to the influx of warmer fluids. In this scenario, hydrocarbons had only limited time to become oxidized, and thus may have only become effectively oxidized in the overlying water column. The intermediate isotopic values, encountered along the mixing line, thus reflect transitional conditions between the two end member conditions of carbonate cementation. In order to further verify this model, additional (trace element) geochemical data are necessary to prove the mixing trend. The occurrence of different organized internal zones indicates that chimney build-up varied through time and space. The nearly identical range of stable isotope data of calcite cemented columns from two different sites, i.e. Slunchevo north and Beloslav Quarry, is interpreted as indication for a fluid source of similar geochemistry, subjected to similar processes of fluid seepage in both areas, i.e. over a distance of at least 4 km.

In total six main levels of horizontal, carbonate cemented interbeds "divide" the vertical arrangement of columns. Both depleted δ^{18}O and δ^{13}C values characterize these interbeds, which differ from a marine signature as expected for classical marine hardgrounds (Bathurst, 1975). In addition, the dominance of a similar interparticle cement phase, i.e. EC1, as encountered in the chimney structures, suggests at least a partial involvement of seepage fluids during horizontal interbed formation. Isotopic ratios of interbeds mostly cluster along the end member of the linear mixing trend of chimneys, with least depleted δ^{13}C and most strongly depleted δ^{18}O values (Fig. 6). In our model, the latter signatures were assumed to indicate pulses of high rate seepage of warm fluids. This suggests that the studied horizontal interbeds near the vertical chimneys, did not merely form during periods of slow and diffuse seepage, as is generally assumed to be responsible for cementation of widespread slabs and concretions at cold seep sites (Kulm and Suess, 1990; Díaz-del-Río et al., 2003). Here, a scenario seemed to be invoked in which mostly fluids, ascending during pulses of faster and active venting affected the isotopic signature of the horizons. However, a single interbed sample with a depleted δ^{13}C of −16‰ V-PDB and oxygen isotopic ratios close to the Lower Eocene marine signature suggest interbed cementation locally also took place during periods of slower (background) seepage. For the basal nummulite-rich hardground, the slight depletion of the carbon and oxygen isotopic ratio with respect to the Lower Eocene marine signature (~50 MA, Zachos et al., 1993), may possibly relate to the limited recrystallization by diffuse upward migrating fluids through the loose, well-sorted, permeable Dikilatash sands. For the subsequent overlying interbed horizons, upward migrating fluids must have been channelled, as diffuse migration was probably blocked by the underlying basal hardground horizon of significant areal extent. Most likely the chimney structures formed the major vertical conduits, but also fracturation of the underlying hardground and interbed levels may have created additional fluid pathways. Additional detailed sampling and analysis of the interbeds in lateral and vertical sense should be carried out, to unravel their exact relation with the vertical chimneys and the reason for their position and repeated occurrence.

As mentioned above, field observations revealed a close relation between the clustered cemented sandstones and NNE–SSW faults. Most settings of active gas seepages reported in literature show that seepage distribution occurs along alignments, controlled by preferential fluid migration paths such as permeable beds or fault zones (Kulm and Suess, 1990; Jorgensen, 1992; Díaz-del-Río et al., 2003). The distribution of gas seeps at the present-day Bulgarian coast seems to be dominantly controlled by specific lineations, e.g. NS to NE–SW oriented faults, outcrops of porous rocks and fronts of active coastal landslides (Dimitrov, 2002). It is highly likely that also the fluids responsible for the formation, close to the seafloor, of the carbonate cemented structures of the Pobiti Kamani area have migrated upward, during Lower Eocene times, along normal fault planes, comparable to the fault observed at Beloslav north (Fig. 1B).

6.2. Process of calcite cementation: bacterially mediated?

Petrographical and geochemical characteristics of the Pobiti Kamani chimneys thus point to an origin related to upward migrating hydrocarbons which become oxidized within the sediment column, resulting in early diagenetic calcite cementation of host sediments, in aerobic conditions close to the sea floor. The aerobic environment, at locations where methane is migrating upward in the sedimentary column, is often typically colonized by bacterial aerobic methanotrophs. These organisms thrive on methane as a carbon source in the presence of free oxygen and produce carbon dioxide and cell-carbon, and live within sediment-pores or in tissues of benthic fauna in a symbiotic association (Madigan et al., 1997; Cavagna et al., 1999). Possibly, their metabolic activity may help to overcome the initial unfavourable conditions of carbonate precipitation upon aerobic methane oxidation (Hovland et al., 1987; Aharon, 2000).

In our petrographical study, only few, fine microbial filaments were locally found, enclosed within column calcite cements (EC1). In order to further investigate possible evidence of fossil bacterial involvement in the cycling of hydrocarbons and the process of calcite cementation, a first reconnaissance study was conducted of lipid biomarkers, based on five samples, derived from chimneys, the basal nummulite-rich hardground and a sample of the host sediment, which served as reference background sample. Preliminary results, however, did not reveal convincing evidence of the presence of known lipid biomarkers of bacterial fauna typically found at cold seeps (Thiel, personal communication). This can possibly be related to diagenetic alteration of the fragile compounds during burial. Based on the assumption made by Botz et al. (1993) of a geothermal gradient of 3 °C/100 m, taking a surface temperature of 10 to 15 °C and the maximum burial depth of 1300 m, possible maximum burial temperatures of 50–55 °C for the Dikilatash sediments can be calculated.

However, when considering the formation mechanism of chimneys at Pobiti Kamani, as addressed above, with regular pulses of fast hydrocarbon seepage, the question raises whether this process of seepage may not have created an unfavourable, possibly too turbulent environment for bacteria to colonize and/or too limited time to actively sequester hydrocarbons and mediate calcite precipitation. An alternative mechanism inducing calcite precipitation may have been the inorganic consumption of interstitial oxygen present in the sediment-pores by ascending reduced hydrocarbon compounds, possibly enhanced, during some periods, by the raised precipitation temperatures, decreasing carbonate solubility.

7. Conclusions

Based on field, petrographical and stable isotope geochemical evidence, the following conclusions can be formulated:

(1) The origin of scattered outcrops of calcite cemented sandstone columns, enveloped in Lower Eocene sands, in the area of Pobiti Kamani (Varna, NE Bulgaria) relates to ancient hydrocarbon seepage. This interpretation is especially based on the depleted δ^{13}C signatures of the authigenic (low-magnesium) calcite cement phase of the column (chimney) structures with values as low as −43‰, ranging up to −25‰, with δ^{18}O of -1 ± 0.5‰ V-PDB.

(2) Stable carbon versus oxygen isotopic signatures of early-diagenetic calcite cemented chimneys from two locations reveal a linear, inverse covariance, with δ^{13}C values (−25‰ to −8‰ V-PDB) increasing with decreasing δ^{18}O (about −1‰ to −8‰ V-PDB). This is qualitatively interpreted as a mixing system of two end member conditions of calcite precipitation, controlled by variable seepage rates of a single hydrocarbon-charged fluid source at depth. During conditions of slow seepage, oxidized methane became the most important contributing carbon source and oxidization occurred within the sediment column in equilibrium with surrounding marine pore water ambient conditions and another end member in which methane was not fully oxidized within the sediment column due to high rates of seepage. Depleted oxygen isotopic signatures of the latter are interpreted in terms of precipitation at elevated temperatures. The proposed model implicates that the fossil seepage system of Pobiti Kamani was not a “cold” seep, sensu stricto. The similarity of this linear trend at the two studied sites at 4 km distance, points to similar seepage processes controlling chimney formation. Furthermore, the presence of an internal pattern along cross-transects of individual chimneys with (concentrically organized) zones of distinct isotopic signature, which vary between the two end member ratios, indicates that seepage-rate controlled precipitation conditions alternated during build-up of individual chimneys.

(3) Six main horizons of horizontal interbeds “divide” the vertical arrangement of chimneys (up to 40 m high). The morphological similarity of the predominant interparticular calcite cement phase within horizontal interbeds compared to chimneys and their range of isotopic signatures of depleted oxygen isotopic ratios and δ^{13}C around −8‰, which approximates the linear mixing trend encountered in chimneys, suggest that fluids responsible for chimney cementation have also contributed to or resetted the cementation of the horizontal interbeds, close to the vertical chimneys. Based on their isotopic ratios, this predominantly occurred during active stages of fluid seepage. The lowermost horizon is distinct regarding its significant areal extent and has been defined as a marine hardground, which is confirmed by its isotopic signature close to the Lower Eocene (~50 MA) marine signature.

(4) The apparent NS alignment of columns at the Beloslav Quarry, the decreasing degree of carbonate cementation in the host sands with distance from the NS oriented major normal fault at the Beloslav north outcrop and in the Beloslav Quarry, together with petrographical indications of the formation of the structures at near surface conditions, suggest a relationship between the distribution of the calcite cemented structures and fluid migration along extensional faults during Lower Eocene times.

(5) In contrast with reported studies from other cold seep sites, only limited petrographical and lipid-biomarker evidence (reconnaissance study) has been found until today within the Pobiti Kamani chimneys, which could form an indication for the presence and possible involvement of known microbial activity in fossil carbon cycling. This may be due to diagenetic alteration of organic compounds during burial. However, considering the processes of fluid seepage controlling chimney growth, as addressed here, the question is raised whether not a process of inorganic hydrocarbon oxidation may have been involved, in which interstitial oxygen was rapidly consumed in reaction with reduced hydrocarbon compounds, without major bacterial mediation.

Acknowledgements

Dr. J. Baccaert, Dr. R. Speijer and Dr. H. Hooyberghs provided comments on paleontology and species identification. Dr. M. Joachimski is thanked for the carbonate stable isotope measurements. The authors are grateful to Dr. V. Thiel for interesting comments on the subject of biogeochemical analyses and for providing results of a reconnaissance lipid-biomarker study. H. Nijs and D. Coetermans are acknowledged for their technical assistance. Dr. P. Clari and an anonymous reviewer are thanked for their constructive review of the manuscript. This study was supported by a research grant from the FWO-Vlaanderen (ESF moundforce G0009.04).

References

Aharon, P., 2000. Microbial processes and products fueled by hydrocarbons at submarine seeps. In: Riding, R.E., Awramik, S.M. (Eds.), Microbial Sediments. Springer-Verlag, Berlin, pp. 270–281.

Aloisi, G., Pierre, C., Rouchy, J.-M., Foucher, J.-P., Woodside, J., MEDINAUT Scientific Party, 2000. Methane-related authigenic carbonates of eastern Mediterranean Sea mud volcanoes and their possible relation to gas hydrate destabilization. Earth and Planetary Science Letters 184, 321–338.

Barneby, R.J., Rimstidt, J.D., 1989. Redox conditions of calcite cementation interpreted from Mn and Fe contents of authigenic calcites. Geological Society of America Bulletin 101, 795–804.

Bathurst, R.G.C., 1975. Carbonate Sediments and their Diagenesis, 2nd edition. Elsevier, Amsterdam.

Bergerat, F., Martin, P., Dimov, D., 1998. The Moesian Platform as a key for understanding the geodynamical evolution of the Carpahto–Balkan alpine system. In: Crasquin-Soleau, S., Barrier, E. (Eds.), Peri-Tethys Memoir 3: Stratigraphy and Evolution of Peri-Tethyan Platforms. Mém. Mus. Natn. Hist. Nat. Ed du Museum Paris, pp. 129–150.

Boetius, A., Ravenschlag, K., Schubert, C.J., Rickert, D., Widdel, F., Gleseke, A., Amann, R., Jorgensen, B.B., Witte, U., Pfannkuche, O., 2000. A marine microbial consortium apparently mediating anaerobic oxidation of methane. Nature 407, 623–626.

Botz, R.W., Georgiev, V., Stoffers, P., Khrischev, Kh., Kostadinov, V., 1993. Stable isotope study of carbonate-cemented rocks from the Pobitite Kamani area, north-eastern Bulgaria. Geologische Rundschau 82, 663–666.

Burton, E.A., 1993. Controls on marine carbonate cement mineralogy: review and reassessment. Chemical Geology 105, 163–179.

Campbell, K.A., Farmer, J.D., Des Marais, D., 2002. Ancient hydrocarbon seeps from the Mesozoic convergent margin of California: carbonate geochemistry, fluids and palaeoenvironments. Geofluids 2, 63–94.

Cavagna, S., Clari, P., Martire, L., 1999. The role of bacteria in the formation of cold seep carbonates: geological evidence from Monferrato (Tertiary, NW Italy). Sedimentary Geology 126, 253–270.

Clari, P.A., Martire, L., 2000. Cold seep carbonates in the tertiary of northwest Italy: evidence of bacterial degradation of methane. In: Riding, R.E., Awramik, S.M. (Eds.), Microbial Sediments. Springer-Verlag, Berlin, pp. 169–261.

Clari, P., Cavagna, S., Martire, L., Hunziker, J., 2004. A miocene mud volcano and its plumbing system: a chaotic complex revisited (Monferrato, NW Italy). Journal of Sedimentary Research 74 (5), 662–676.

Díaz-del-Río, V., Somoza, L., Martínez-Frias, J., Mata, M.P., Delgado, A., Hernandez-Molina, F.J., Lunar, R., Martín-Rubí, J.A., Maestro, A., Fernández-Puga, M.C., Léon, R., Llave, E., Medialdea, T., Vázqiez, J.T., 2003. Vast fields of hydrocarbon-derived carbonate chimneys related to the accretionary wedge/olistostrome of the Gulf of Cádiz. Marine Geology 195, 177–200.

Dimitrov, L., 2002. Contribution to atmospheric methane by natural seepages on the Bulgarian continental shelf. Continental Shelf Research 22, 2429–2442.

Dimitrov, L., Dontcheva, V., 1994. Seabed pockmarks in the southern Bulgarian Black Sea zone. Bulletin of the Geological Society of Denmark 41, 24–33.

Doglioni, C., Busatta, C., Bolis, G., Marianini, L., Zanella, M., 1996. Structural evolution of the eastern Balkans (Bulgaria). Marine and Petroleum Geology 13 (2), 225–251.

Flügel, E., 2004. Microfacies of carbonate rocks. Analysis, Intrepretation and Application. Springer Berlin, Heidelberg.

Foose, M., Manheim, F., 1975. Geology of Bulgaria: a review. The American Associations of Petroleum Geologists Bulletin 59 (2), 303–335.

Galehouse, J.S., 1971. Point counting. In: Carver, R.E. (Ed.), Procedures in Sedimentary Petrology. John Wiley and Sons, New York, pp. 385–407.

Greinert, J., Bohrmann, G., Suess, E., 2001. Gas hydrate-associated carbonates and methane-venting at hydrate ridge: classification, distribution and origin of authigenic lithologies. In: Paull, C.K., Dillon, W.P. (Eds.), Natural Gas Hydrates Occurrence, Distribution and Detection. American Geophysical Union, Washington DC, pp. 99–113.

Hoehler, T.M., Alperin, M.J., Albert, D.B., Martens, C.S., 1994. Field and laboratory studies of methane oxidation in an anoxic marine sediment. Evidence for a methanogen-sulfate reducer consortium. Global Biogeochemical Cycles 8 (4), 451–463.

Hovland, M., Talbot, M.R., Qvale, H., Olaussen, S., Aasberg, L., 1987. Methane-related carbonate cements in pockmarks of the North Sea. Journal of Sedimentary Petrology 57 (5), 881–892.

Hsü, K.J., Nachev, I.K., Vuchev, V.T., 1977. Geologic evolution of Bulgaria in light of plate tectonics. Tectonophysics 40, 245–256.

Hudson, J.D., 1977. Stable isotopes and limestone lithification. Journal of the Geological Society of London 133, 637–660.

Jensen, P., Aagaard, I., Burke, R.A. Jr., Dando, P.R., Jorgensen, N.O., Kuijpers, A., Laier, T., O'Hara, S.C.M., Schamaljohann, R., 1992. 'Bubbling reefs' in the Kattegat: submarine landscapes of carbonate-cemented rocks support a diverse ecosystem at methane seeps. Marine Ecology Progress Series 83, 103–112.

Jorgensen, N.O., 1992. Methane-derived carbonate cementation of marine sediments from the Kattegat, Denmark: geochemical and geological evidence. Marine Geology 103, 1–13.

Kulm, L.V.D., Suess, E., 1990. Relationship between carbonate deposits and fluid venting: Oregon accretionary prism. Journal of Geophysical Research 95 (B6), 8899–8915.

Madigan, M.T., Martinko, J.M., Parker, J., 1997. Brock Biology of Microorganisms, 8th edition. Prentice-Hall, Inc., New Jersey.

Michaelis, W., Seifert, R., Nauhaus, K., Treude, T., Thiel, V., Blumenberg, M., Knittel, K., Gieseke, A., Peterknecht, K., Pape, T., Boetius, A., Amann, R., Jorgensen, B.B., Widdel, F., Peckmann, J., Pimenov, N.V., Gulin, M.B., 2002. Microbial reefs in the Black Sea fueled by anaerobic oxidation of methane. Nature 297, 1013–1015.

Nacev, I., Mandev, P., Zhelev, S., 1986. "Pobitite Kamani" — algal bioherms. Reviews Bulletin of the Geological Society 47, 1–13 (in Bulgarian, English summary).

Peckmann, J., Thiel, V., 2004. Carbon cycling at ancient methane-seeps. Chemical Geology 205 (3–4), 443–467.

Peckmann, J., Thiel, V., Michaelis, W., Clari, P., Gaillard, C., Martire, L., Reitner, J., 1999. Cold seep deposits of Beauvoisin (Oxfordian; southeastern France) and Marmorito (Miocene; northern Italy): microbially induced authigenic carbonates. International Journal of Earth Sciences 88, 60–75.

Peckmann, J., Reimer, A., Luth, U., Hansen, B.T., Heinicke, C., Hoefs, J., Reitner, J., 2001. Methane-derived carbonates and authigenic pyrite from the northwestern Black Sea. Marine Geology 177, 129–150.

Peckmann, J., Goedert, J.L., Thiel, V., Michaelis, W., Reitner, J., 2002. A comprehensive approach to the study of methane-seep deposits from the Lincoln Creek Formation, western Washington State, USA. Sedimentology 49, 855–873.

Ritger, S., Carson, R., Suess, E., 1987. Methane-derived authigenic carbonates formed by subduction-induced pore-water expulsion along the Oregon/Washington margin. Geological Society of America Bulletin 98, 147–156.

Sakai, H., Gamo, T., Ogawa, Y., Boulegue, J., 1992. Stable isotopic ratios and origins of the carbonates associated with cold seepage at the eastern Nankai Trough. Earth and Planetary Science Lettres 109, 391–404.

Stakes, D.S., Orange, D., Paduan, J.B., Salamy, K.A., Maher, N., 1999. Cold-seeps and authigenic carbonate formation in Monterey Bay, California. Marine Geology 159, 93–109.

Thiel, V., Peckmann, J., Seifert, R., Wehrung, P., Reitner, J., Michaelis, W., 1999. Highly isotopically depleted isoprenoids: molecular markers for ancient methane venting. Geochimica et Cosmochimica Acta 63 (23/24), 3959–3966.

Thiel, V., Peckmann, J., Richnow, H.H., Luth, U., Reitner, J., Michaelis, W., 2001. Molecular signals for anaerobic methane oxidation in Black Sea seep carbonates and a microbial mat. Marine Chemistry 73, 97–112.

Wachter, E., Hayes, J.M., 1985. Exchange of oxygen isotopes in carbon dioxide–phosphoric acid systems. Chemical Geology 52, 365–374.

Zachos, J.C., Lohmann, K.C., Walker, J.C.G., Wise, S.W., 1993. Abrupt climate change and transient climates during the Paleogene: a marine perspective. Journal of Geology 101, 191–213.